PNAS RESEARCH ARTICLE | NEUROSCIENCE

Hemispheric asymmetry in cortical thinning reflects intrinsic organization of the neurotransmitter systems and homotopic functional connectivity

Zhijie Liao[a,b], Tobias Banaschewski[c], Arun L. W. Bokde[d,e], Sylvane Desrivières[f], Herta Flor[g,h], Antoine Grigis[i], Hugh Garavan[j,k], Penny Gowland[l], Andreas Heinz[m], Bernd Ittermann[n], Jean-Luc Martinot[o], Marie-Laure Paillère Martinot[o,p], Eric Artiges[o,q], Frauke Nees[c,g,r], Dimitri Papadopoulos Orfanos[i], Luise Poustka[s], Sarah Hohmann[c], Sabina Millenet[c], Juliane H. Fröhner[t], Michael N. Smolka[t], Henrik Walter[m], Robert Whelan[u], Gunter Schumann[v,w], Tomáš Paus[a,b,x,1], and IMAGEN Consortium

Edited by Anna C. (Kia) Nobre, Yale University, New Haven, CT; received April 28, 2023; accepted September 7, 2023

Hemispheric lateralization and its origins have been of great interest in neuroscience for over a century. The left–right asymmetry in cortical thickness may stem from differential maturation of the cerebral cortex in the two hemispheres. Here, we investigated the spatial pattern of hemispheric differences in cortical thinning during adolescence, and its relationship with the density of neurotransmitter receptors and homotopic functional connectivity. Using longitudinal data from IMAGEN study (N = 532), we found that many cortical regions in the frontal and temporal lobes thinned more in the right hemisphere than in the left. Conversely, several regions in the occipital and parietal lobes thinned less in the right (vs. left) hemisphere. We then revealed that regions thinning more in the right (vs. left) hemispheres had higher density of neurotransmitter receptors and transporters in the right (vs. left) side. Moreover, the hemispheric differences in cortical thinning were predicted by homotopic functional connectivity. Specifically, regions with stronger homotopic functional connectivity showed a more symmetrical rate of cortical thinning between the left and right hemispheres, compared with regions with weaker homotopic functional connectivity. Based on these findings, we suggest that the typical patterns of hemispheric differences in cortical thinning may reflect the intrinsic organization of the neurotransmitter systems and related patterns of homotopic functional connectivity.

hemispheric asymmetry | cortical thickness | adolescence | neurotransmitters | plasticity

Hemispheric asymmetries in the structure and function of the human brain have been a fascinating topic for scientists for over a century. Several hypotheses have been proposed to explain the origin of structural asymmetries between the left and right hemispheres, including genetic factors and developmental processes during the prenatal and postnatal periods (1–3). The typical spatial pattern of hemispheric asymmetry in thickness of the human cerebral cortex emerges during postnatal development (4–6). From birth to childhood and throughout adolescence, asymmetry in cortical thickness changes continuously, as a result of differences in cortical maturation between the left and right hemispheres (4–6). For instance, in early childhood, the orbitofrontal and inferior frontal regions in the left hemisphere are thicker than those on the right (5). This (L>R) asymmetry reverses in late adolescence because the regions on the left thinned more than those on the right during this developmental period (5). In patients with attention-deficit/hyperactivity disorder, these typical left–right differences in cortical thinning appear to be absent, resulting in altered asymmetry patterns observed in adulthood (5, 7). Therefore, understanding the mechanisms underlying the typical hemispheric differences in thinning during development can provide insights into abnormal asymmetry patterns in neurodevelopmental disorders. Mechanisms underlying the hemispheric differences in thinning are still largely unknown, however.

The pattern of hemispheric differences in cortical thinning may be structured along general principles of cortical organization (e.g., refs. 8 and 9). Here, we investigate whether hemispheric differences in thinning are associated with the (intrinsic) organization of the neurotransmitter–receptor system. The density of various neurotransmitter receptors vary across cortical regions, and are associated with spatial gradients in various microscopic (e.g., cyto- and myelo-architecture) and macroscopic (e.g., diffusion-based tractography) features (10–12). The spatial correlation between densities of neurotransmitter receptors and other structural features across the human cerebral cortex suggests that the organization of the neurotransmitter receptors system may reflect an intrinsic organization of the cortex that, in turn, may determine the developmental trajectory of cortical thickness and

Significance

Hemispheric asymmetry of the human cerebral cortex is a long-standing issue, and the asymmetry in cortical thickness is thought to stem from hemispheric differences in cortical maturation. Nevertheless, the mechanisms of the asymmetric maturation remain unknown. Here, with a longitudinal cohort, we revealed that the spatial pattern of hemispheric differences in cortical thinning during adolescence reflect the hemispheric differences in the density of neurotransmitter receptors and transporters. Moreover, regions with stronger homotopic functional connectivity had a more symmetrical rate of cortical thinning and density of neurotransmitter receptors and transporters between the left and right hemispheres. These findings point to a structure–function interaction as a possible mechanism underlying the prototypical pattern in the hemispheric differences in cortical thinning.

This article is a PNAS Direct Submission.

[1]To whom correspondence may be addressed. Email: tpausresearch@gmail.com.

This article contains supporting information online at https://www.pnas.org/lookup/suppl/doi:10.1073/pnas.2306990120/-/DCSupplemental.

Published October 13, 2023.

its hemispheric asymmetry. Therefore, we hypothesized that the left–right differences in the density of neurotransmitter receptors could reflect the pattern of hemispheric differences in cortical thinning during adolescence.

Homotopic functional connectivity, as manifested by temporal cooccurrence of neuronal activity between the left–right homotopic regions, may also relate to the hemispheric differences in cortical thinning during adolescence. This possibility is supported by experimental evidence of activity-dependent structural plasticity in the cerebral cortex (13–15). For example, learning to juggle or to play music could induce structural changes in the cerebral cortex (13, 16). Similarly, if the left and right homotopic regions engage concurrently during the performance of tasks (i.e., strong functional connectivity), they may display a similar rate of cortical thinning during development. In contrast, the left and right homotopic regions with low homotopic functional connectivity between them may thin at different rates. It has been shown that, on a group-average level, functional connectivity can predict whether a pair of cortical regions thin similarly during adolescence (17). This finding was derived by comparing the similarity in cortical thinning rates between predefined pairs of regions with strong functional connectivity, including homotopic connectivity, against other pairs of regions (17). Furthermore, an individual's interregional profile of functional connectivity is shaped by both the intrinsic organization principles (shared across individuals) and the individual-specific (nonshared) characteristics (18, 19). It is therefore important to distinguish the relative contribution of the individual-shared and individual-specific characteristics in the relationship between functional connectivity and the hemispheric differences in cortical thinning.

Here, we used data obtained in a longitudinal study, namely IMAGEN (20), to investigate hemispheric differences in cortical thinning and its underlying mechanisms. Incorporating data on the density of neurotransmitter receptors and transporters (12), we investigated whether the typical pattern of hemispheric differences in cortical thinning was related to the hemispheric differences in the density of neurotransmitter receptors/transporters. Further, we tested our hypothesis that cortical regions with stronger homotopic functional connectivity during adolescence would demonstrate smaller hemispheric differences in thinning, as compared with regions with weaker homotopic functional connectivity; we predicted that this would be the case at both the group-average and individual levels.

Results

Left–Right Differences in Cortical Thinning and the Maturation of Thickness Asymmetry. First, we examined differences in cortical thinning during adolescence between the left and right hemispheres using data from the IMAGEN study. There were 532 participants (310 females) who had high-quality T1-weighted and functional magnetic resonance imaging (MRI) datasets at all three visits (visit 1: 14 y, visit 2: 19 y, and visit 3: 22 y; see *Methods* for details). For each participant, we calculated the rate of cortical thinning from visit 1 to visit 3 for 68 cortical regions (34 per hemisphere) segmented by FreeSurfer using the Desikan–Killiany atlas (21).

We found that, from adolescence to adulthood, the magnitude and direction of hemispheric differences in cortical thinning varied across regions (Fig. 1*A* and *SI Appendix*, Table S1). Specifically, many regions in the frontal and temporal lobes exhibited greater thinning in the right (vs. left) hemisphere. On the other hand, several regions in the occipital and parietal lobes thinned less in the right (vs. left) hemisphere (Fig. 1*A* and *SI Appendix*, Table S1). This spatial pattern of hemispheric differences in thinning is

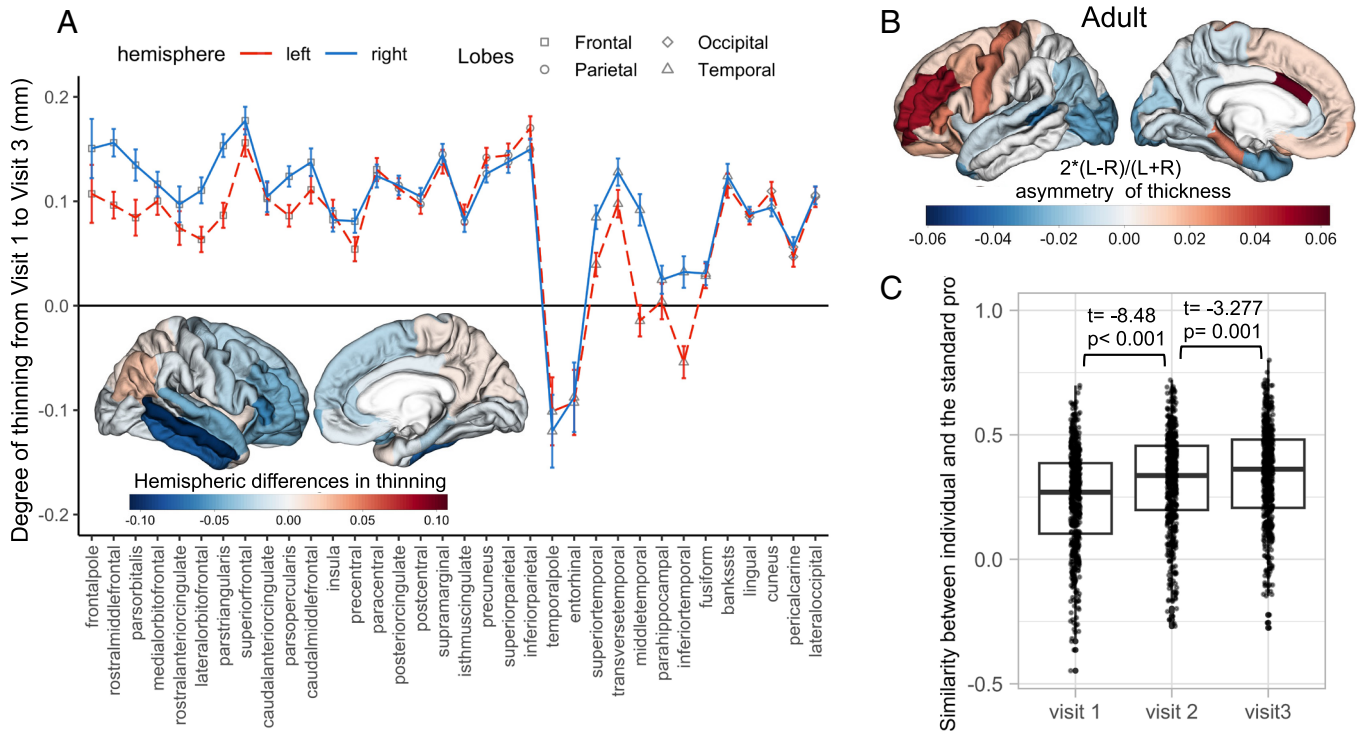

Fig. 1. Hemispheric differences in cortical thinning and the maturation of thickness asymmetry. (*A*) The degree of cortical thinning (higher values, more thinning) from visit 1 to visit 3 in the left and the right hemispheres (plot), and the map of hemispheric differences in thinning (*Left Bottom*). The error bars in Fig. 1*A* represent the 95% CI of cortical thinning within each region. In the brain map, negative values (in blue) of hemispheric differences in thinning indicate more thinning in the right than the left hemisphere. (*B*) The adult profile of thickness asymmetry was derived from 231 young adults, positive values (in red) indicate the left hemisphere is thicker than the right. (*C*) From adolescence to adulthood, individual profiles of thickness asymmetry became more similar to the adult profile.

related to the maturation of hemispheric asymmetry in cortical thickness. Thus, the overall spatial pattern of thickness asymmetry, defined as (Left–Right)/(0.5*(Left + Right)), became more similar to an adult profile: multiple regions in the frontal lobe were thinner in the right (vs. left) hemisphere, while many regions in the occipital and temporal lobes were thicker in the right (vs. left) hemisphere (Fig. 1 *B* and *C*). The adult profile of hemispheric asymmetry in cortical thickness was derived by averaging thickness-asymmetry profiles of an independent set of participants aged 22 y from IMAGEN (N = 231, Fig. 1*B*). The similarity (Pearson correlation) between individual profiles and the adult profile increased on average from r = 0.240 at visit 1 to r = 0.311 at visit 2, and to r = 0.338 at visit 3 (Fig. 1*C*). We also observed a comparable increase in the similarity between individual profiles and the profile of average thickness asymmetry based on 17,141 individuals from the ENIGMA study (22; *SI Appendix*, Fig. S1).

Left–Right Differences in Neurotransmitter Receptors and Left–Right Differences in Thinning. In order to identify possible mechanisms underlying the observed hemispheric differences in cortical thinning, we investigated whether these differences were associated with hemispheric differences in the density of neurotransmitter receptors and transporters. First, we obtained a group-average profile of hemispheric differences in cortical thinning, where positive values mean greater thinning in the left hemisphere compared with the right hemisphere (Fig. 2). We then derived profiles of hemispheric differences (Left–Right) in the density for each of 19 neurotransmitter receptors and transporters using data acquired with positron emission tomography (PET) (12 and Dataset S1). Positive values in these profiles indicate greater receptor density in the left (vs. right) hemisphere. We then examined the relationship between the profile of hemispheric differences in cortical thinning and the profile of hemispheric differences in density for each of the 19 neurotransmitter receptors/transporters using simple permutation tests (*Methods*). Since spatial autocorrelation gains rising attention, we conducted additional permutation tests to adjust for spatial autocorrelation using Brain Surrogate Maps with Autocorrelated Spatial Heterogeneity (BrainSMASH). Note, however, that spatial autocorrelation in brain maps can be attributed to regional similarities in biological processes, such as development and neuronal connectivity (23, 24). As such, adjusting spatial autocorrelation may attenuate true relationships. We reported results from both permutation approaches.

Our results showed that the hemispheric differences in neurotransmitter receptor/transporters density were generally positively associated with the hemispheric differences in cortical thinning, with 8 (7 with BrainSMASH) out of the 19 receptors showing statistically significant relationships after false discovery rate (FDR) correction (Fig. 2 and Table 1). These receptors included NMDA, DAT, MOR, 5HT1b, VAChT, D1, mGluR5, and NET. Specifically, many regions in the frontal and temporal lobes had higher receptor/transporter density in the right (vs. left) hemisphere, and these regions showed

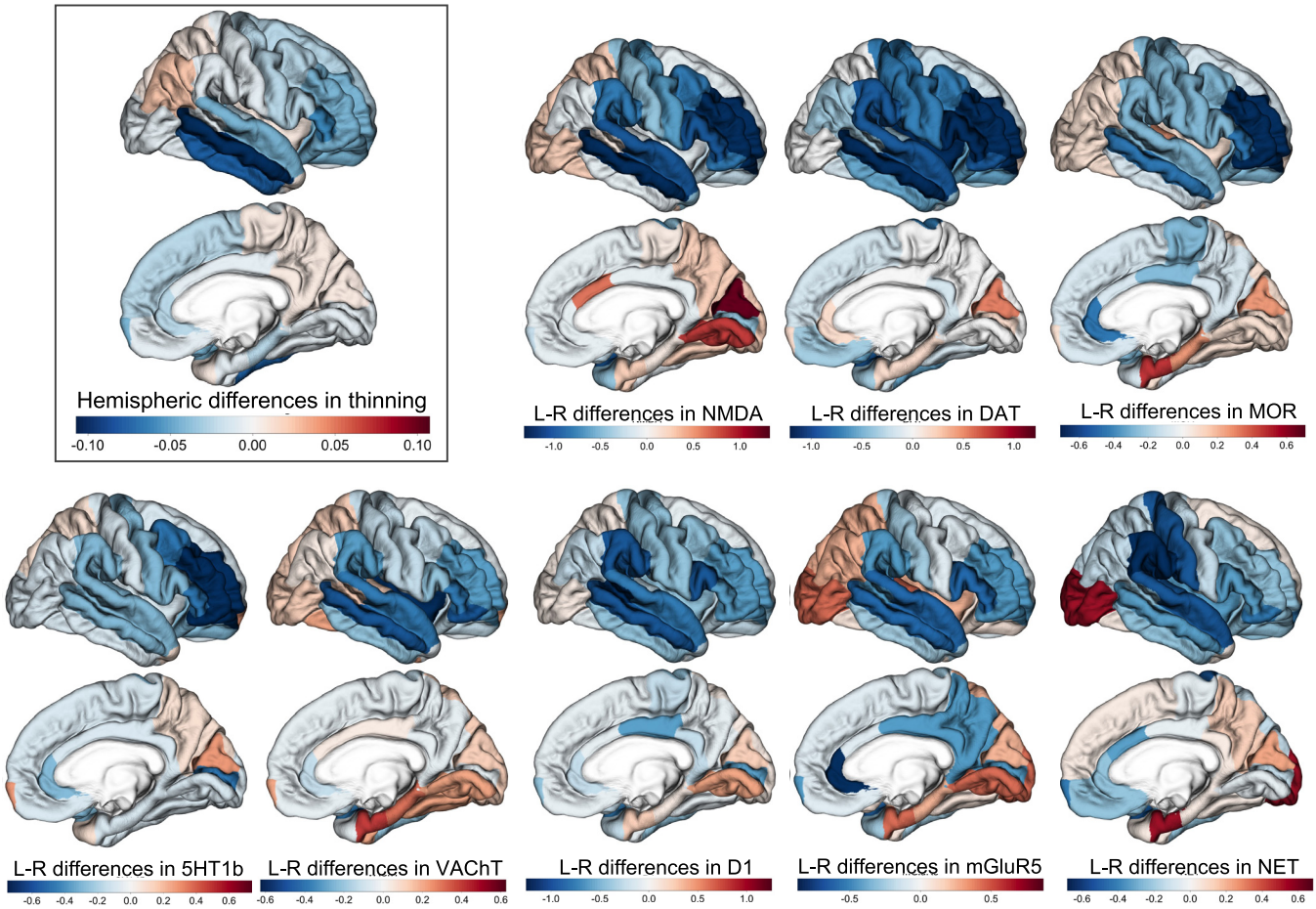

Fig. 2. The hemispheric differences in neurotransmitter receptor/transporter density reflect the left–right differences in cortical thinning during adolescence. Negative values of hemispheric differences in cortical thinning mean more thinning in the right vs. left hemisphere during adolescence. Similarly, negative values of hemispheric (L-R) differences in density mean denser receptors/transporters in the right vs. left hemisphere. Regions that have a higher density of neurotransmitter receptors/transporters in the right (vs. left) showed more thinning in the right (vs. left) hemisphere. The results are projected onto a right-hemispheric template since more regions are right-dominant in thinning and the density of neurotransmitter receptors.

Table 1. Results of correlations between the hemispheric differences in thinning and the left–right differences in receptor/transporter density

receptor/transporter	correlation (r)	r^2	*P* value	*P*.fdr	*P* value (BrainSMASH)	*P*.fdr (BrainSMASH)
NMDA	0.6324	0.3999	0.0001	0.0019	0.0005	0.0095
DAT	0.5323	0.2833	0.0008	0.0076	0.0087	0.0358
MOR	0.5221	0.2726	0.0014	0.0089	0.0101	0.0358
VAChT	0.5080	0.2581	0.0023	0.0109	0.0057	0.0358
5HT1b	0.4667	0.2178	0.0058	0.0184	0.0037	0.0352
D1	0.4630	0.2144	0.0051	0.0184	0.0113	0.0358
mGluR5	0.4275	0.1827	0.0099	0.0269	0.0174	0.0472
NET	0.4129	0.1705	0.0164	0.0389	0.0437	0.1038
GABAa	0.3729	0.1391	0.0291	0.0614	0.0628	0.1193
5HT1a	0.3545	0.1256	0.0394	0.0749	0.0613	0.1193
M1	0.3462	0.1199	0.0451	0.0779	0.0858	0.1427
5HT6	−0.2691	0.0724	0.1237	0.1958	0.0901	0.1427
H3	0.2031	0.0413	0.2404	0.3513	0.4425	0.5255
5HT4	0.1936	0.0375	0.2721	0.3692	0.3051	0.4437
5HT2a	0.1810	0.0328	0.3069	0.3887	0.3503	0.4437
5HTT	0.1581	0.0250	0.3681	0.4371	0.3499	0.4437
D2	0.1057	0.0112	0.5483	0.6129	0.6759	0.7554
CB1	−0.0279	0.0008	0.8752	0.9238	0.8905	0.9400
α4β2	−0.0134	0.0002	0.9380	0.9380	0.9470	0.9470

The 19 receptors/transporters are listed in the order of the effect size (r^2).

more thinning in the right (vs. left) hemisphere during adolescence (Fig. 2). In contrast, many regions in the parietal and occipital lobes had lower receptor/transporter density in the right (vs. left) hemisphere, and these regions thinned less in the right (vs. left) hemisphere (Fig. 2). Note that the top and bottom five neurotransmitter receptors/transporters shown in Table 1 show differences in their gene coexpression networks in the human cerebral, with their coexpressed genes being associated with distinct biological processes according to Gene Ontology enrichment analysis (*SI Appendix*, Fig. S3).

Homotopic Functional Connectivity and Left–Right Differences in Thinning during Adolescence. Next, we investigated whether regions exhibiting strong homotopic functional connectivity demonstrate similar cortical thinning during adolescence. Given that homotopic functional connectivity is undirected, to test this hypothesis, we used the absolute values of hemispheric differences in thinning and referred to it as "absolute hemispheric differences in thinning". Homotopic functional connectivity was derived from functional MRI datasets obtained while participants watched video clips of faces and nonbiological motion in three visits, as outlined in the Methods section. We conducted permutation tests (with and without spatial autocorrelation) to analyze correlation—across the 34 cortical regions—between the homotopic functional connectivity and the absolute hemispheric differences in thinning at both the group-average and individual levels (*Methods*).

At the group-average level, we found a negative correlation between homotopic functional connectivity and absolute hemispheric differences in thinning (r = –0.408, *P* = 0.009, *P*-BrainSMASH = 0.032. Fig. 3*A*). These results indicate that regions with strong homotopic functional connectivity exhibit similar degrees of thinning between the left and right hemispheres, whereas regions with weaker homotopic functional connectivity display greater differences in cortical thinning between the two hemispheres.

At the individual level, we also found negative correlations between individuals' functional connectivity and their own absolute-hemispheric differences in thinning profiles (correlation coefficients, mean = –0.393, SD = 0.138, *P* < 2.2E–16, *P*-BrainSMASH < 2.2E–16). Next, we sought to determine whether the pattern of absolute hemispheric differences in thinning was influenced by the individual-specific or individual-shared components of homotopic functional connectivity. This was tested by comparing the correlations of absolute hemispheric differences in thinning and functional connectivity profiles within individuals ("intraindividual" correlations) to those between individuals ("interindividual" correlations). The assumption tested here is that if the individual-specific component of homotopic functional connectivity contributed to the pattern of absolute hemispheric differences in thinning, then participants' functional connectivity profiles would predict their own absolute hemispheric differences in thinning profiles better compared with those of other individuals. This was not the case: we found no significant differences between intra- and inter-individual correlations (paired *t* test: t = 0.863, *P* = 0.389, *SI Appendix*, Fig. S2).

Finally, the hemispheric differences in neurotransmitter receptors and transporters might relate to functional lateralization that, in turn, influences the hemispheric difference in thinning. To test this possibility, we assessed whether regions with high hemispheric differences in the density of neurotransmitter receptors and transporters displayed weaker homotopic functional connectivity, as compared with regions with low hemispheric differences in the neurotransmitter systems. We derived a profile called "neurotransmitter differences" by summing up the absolute hemispheric differences in the density of 19 neurotransmitter receptors/transporters for each of the 34 regions. We found that regions with higher neurotransmitter differences between the two hemispheres had weaker homotopic functional connectivity (r = –0.334, *P* = 0.028, *P*-BrainSMASH = 0.095, Fig. 3*B*).

Discussion

In this study, we revealed that the spatial (interregional) pattern of hemispheric differences in cortical thinning during adolescence,

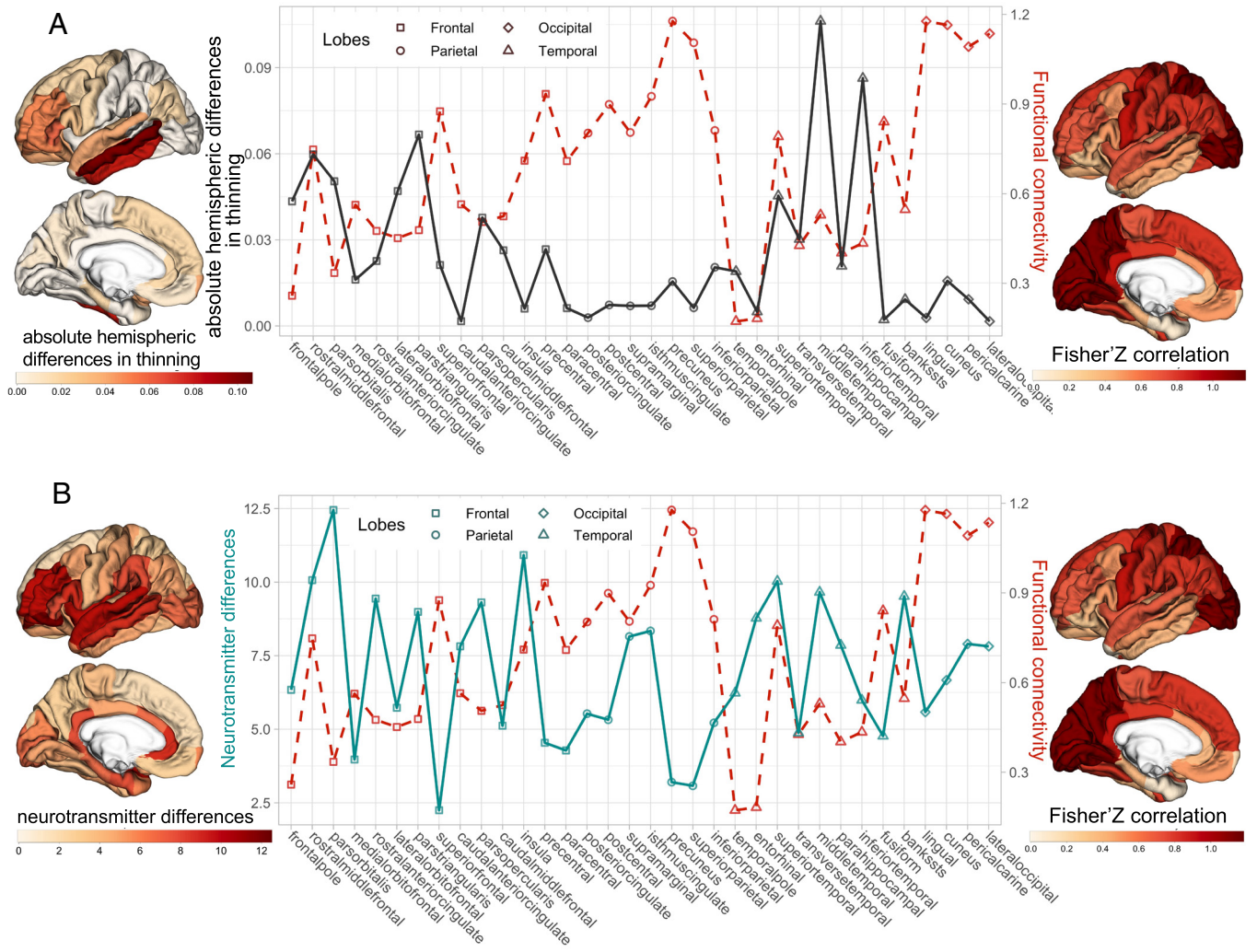

Fig. 3. Relationship between homotopic functional connectivity and the hemispheric differences in thinning during adolescence. (*A*) The profile of group-averaged absolute hemispheric difference in thinning during adolescence (on the left, black solid line) and the group-averaged homotopic functional connectivity (on the right, red dash line). The higher value of absolute hemispheric difference in thinning, the more differences in cortical thinning between the left and right hemispheres. (*B*) The profile of the neurotransmitter differences (on the left, cyan solid line) and the group-averaged homotopic functional connectivity. The higher value of the receptor differences, the more differences in the density of neurotransmitter receptors and transporters between the left and right hemispheres.

which led to the maturation of thickness asymmetry, was reflected in hemispheric differences in the density of neurotransmitter receptors and transporters. We also found that regions with stronger homotopic functional connectivity had more similar rate of cortical thinning as well as density of neurotransmitter receptors and transporters between the left and right hemispheres.

From adolescence to adulthood, many frontal and temporal regions thinned more in the right than the left hemisphere, while a few occipital and parietal regions show the opposite pattern. As a result of these left–right differences in thinning, by young adulthood, most of the frontal regions are thicker in the left vs. right hemisphere (i.e., L > R), with a few regions in the occipital and parietal lobes showing the opposite pattern (i.e., R > L). Thus, at this point of cortical maturation, the overall spatial pattern of hemispheric asymmetry in cortical thickness becomes similar to that observed in adults. The pattern of left–right differences in cortical thinning and age-related changes in thickness asymmetry observed here are inconsistent with previous studies. For example, Zhou et al. and Shaw et al. showed smaller age-related decreases in cortical thickness in the right than the left hemisphere in some frontal regions, and larger age-related decreases in thickness of posterior temporo-occipital regions in the right than the left (5, 6). Unlike the current report, however, these reports relied on a mixed (cross-sectional and longitudinal) design that included individuals in a broad age range (3 to 22 y of age). Nonetheless, consistent with these studies, our findings suggest that the spatial pattern of thickness asymmetry becomes closer to the typical adults' profile during postnatal development. This is confirmed not only with our (IMAGEN) dataset but also with the population-average obtained in 17,141 healthy individuals from the ENIGMA Consortium (22). Our finding indicates that the hemispheric differences in thinning and the maturation of individuals' thickness asymmetry may, at least in part, follow a prototypical (spatial) pattern shared across individuals. Disruptions of such a prototypical pattern of the left–right differences in cortical thinning may contribute to the abnormal hemispheric asymmetries found in patients with psychopathology (5, 25).

Importantly, we revealed a link between the hemispheric asymmetries in cortical thinning and the density of neurotransmitter receptors/transporters. In addition, we found that regions with large hemispheric differences in both the rate of cortical thinning and the density of neurotransmitter receptors and transporters are those with weak homotopic functional connectivity. Taken together, our findings point to a structure–function interaction

as a possible mechanism underlying the prototypical pattern in the hemispheric differences in cortical thinning. Neurotransmitter receptors are primarily located on dendritic spines, which are crucial for synaptic transmission and modulations (26). Interregional variations in the density of neurotransmitter receptors in the cerebral cortex, or regional chemoarchitecture, reflect regional differences in cyto- and myelo-architecture, as well as brain functions (10, 27). Genes coexpressed with the genes of neurotransmitter receptors/transporters that showed the strongest relationships with the asymmetrical thinning are enriched in biological processes of synaptic signaling, synapse organization, and learning (*SI Appendix*, Fig. S3). Notably, the NMDA receptor, which exhibited the strongest relationship with hemispheric differences in cortical thinning, is known to play a role in regulating dendritic growth and synaptic plasticity (28, 29). Note that within 1 mm^3 of the human cerebral cortex, dendrites account for roughly 26% of the volume and contain approximately 150 million synapses (26). Any changes of these cellular components may influence MRI signals and thus, affect the measure of cortical thickness (30, 31). Our previous studies have revealed a spatial relationship between age-related cortical thinning during childhood and adolescence and the expression of genes related to pyramidal cells and the regulation of dendritic extensions (30, 32, 33). This evidence places the dendrites and synapses at the crossroad between function (neuronal activity) and structure (cortical thickness) through activity-dependent neuronal plasticity. Thus, regions with hemispheric differences in their chemoarchitecture may also exhibit dissimilarities in activity-related remodeling of dendritic arbors and intracortical myelination via neuronal plasticity (13, 15, 34). This, in turn, would lead to hemispheric differences in cortical thinning during adolescence, as observed here and previously (30–33). Alternatively, since age-related cortical thinning coincides with pruning of synapses and dendrites (35), it is also possible that asymmetry in the density of neurotransmitter receptor/transporter, as observed in the adult cerebral cortex, can be a consequence of the age-related loss of synapse and dendrites. This is not very likely, however. Out of the 23 neurotransmitter receptors/transporter genes, age showed no correlation with the expression of 13 genes, and it explained only a small proportion of variance (r^2: 0.015 to 0.065) in the expression of the remaining 10 genes (*SI Appendix*, Table S2 and Fig. S4). Furthermore, the observed positive relationship between the hemispheric asymmetry in cortical thinning (more in the right vs. left hemisphere) and that in the receptor/transport density (higher in the right vs. left hemisphere) provides further evidence against the possibility that the density is a consequence of the thinning. Nonetheless, it is important to note that the observed structure–function associations may involve multiple levels of cause–effect relationships, which cannot be inferred from the purely correlational observations reported here.

Overall, our observations are consistent with the notion of an intrinsic organization of the cerebral cortex as the main driver of the spatial organization of different neural systems and developmental processes. These intrinsic—or prototypical—are shared by all individuals. Others have observed such spatial covariances across multiple in vivo (e.g., functional connectivity and cortical thinning) and ex vivo (e.g., cytoarchitecture) phenotypes (17, 36, 37). While we postulate a structure–function interaction as a potential mechanism underlying the prototypical pattern of the hemispheric differences in cortical thinning, caution should be taken in drawing conclusions about causality, as the observed relationships are only correlational in nature. It is possible that a third party, such as genetic similarities and dissimilarities, give rise to the convergence between the brain function and structure. In addition, while individuals share these prototypical (spatial) patterns, we know very little about factors (internal or external) that may drive individual variability in hemispheric asymmetries, both structural and functional. Twin and genome-wide association studies revealed low heritability of the hemispheric asymmetry in cortical thickness, suggesting that its developmental mechanisms are tightly constrained and largely genetically invariant in the population, and environmental factors and developmental randomness may be primarily responsible for the individual variability of this phenotype (38, 39). Future studies with multimodal brain imaging and omics data at the individual level may help elucidate the factors contributing to the prototypical and individual-varied patterns of brain lateralization and ultimately lead to a better understanding of abnormal asymmetry observed in neurodevelopmental disorders.

Method

Participants. The IMAGEN Study is a longitudinal study that, at baseline, recruited a community-based sample of 2,000 adolescents, 13 to 15 y of age, at eight sites located in England (London, Nottingham), France (Paris), Ireland (Dublin), and Germany (Berlin, Dresden, Hamburg, and Mannheim) (20). Further details are available at https://imagen-project.org/the-imagen-dataset/. We used data from 532 participants (female = 310, male = 222) with high-quality structural and functional MRI data available at all three visits: visit 1, visit 2, and visit 3 at age of 14 y (Mean ± SD: 14.46 ± 0.39), 19 y (19.15 ± 0.78), and 22 y (22.02 ± 0.64), respectively.

MRI Acquisition and Processing. In IMAGEN, high-resolution T1-weighted images and functional images were obtained with 3-Tesla MRI systems from different manufacturers (Siemens: five sites, Philips: two sites, and General Electric: one site). Briefly, T1-weighted anatomical images were acquired using three-dimensional magnetization-prepared rapid acquisition with gradient echo (3D MPRAGE) sequences (resolution = 1.1 × 1.1 × 1.1 mm) based on ADNI protocol (https://adni.loni.usc.edu/methods/documents/mri-protocols/). Functional images were acquired with gradient echo-echo planar imaging (GE-EPI) sequences (resolution = 3.4 × 3.4 mm; slice thickness = 2.4 mm; TR = 2,200 ms; TE = 30 ms). Detailed MR protocol and cross-site standardization of the IMAGEN study can be found in IMAGEN Github (https://github.com/imagen2). During the functional MRI session, participants viewed passively short video clips displaying dynamic ambiguous facial expressions, angry facial expression, or nonbiological control stimuli. The control stimuli consisted of black-and-white concentric circles of various contrasts, expanding and contracting at various speeds. The three viewing conditions were organized into 19 blocks of 18s duration each (5 ambiguous, 5 angry, and 9 control) for a single 6 min functional MRI run (details can be found in the initial report describing this paradigm) (40). Quality control, preprocessing of anatomical and functional data were performed, respectively, with MRIQC 0.15.0 (41), fMRIPrep 1.3.2 (42), and FSL_regfilt 5.0.9. More details have been described in previous study (19).

Mean cortical thickness was extracted for each of the 68 regions (34 per hemisphere) in the Desikan–Killiany atlas (21) through the FreeSurfer (v6.0.0) implemented in the fMRIPrep pipeline. ComBat was used to harmonize the cortical thickness measurements across scanners and sites at each visit (43). The cortical thinning from visit 1 to visit 3 was calculated for each region and each participant. Thus, a higher value of cortical thinning means more decreases in cortical thickness during adolescence. Additionally, for each visit and each participant, the thickness asymmetry was calculated for each pair of left–right homotopic regions using the formula: (left − right)/((left + right)*0.5). Given this definition, a positive value of thickness asymmetry reflects leftward asymmetry (L > R). The same cortical parcellation was applied to functional images to extract mean blood-oxygen-level-dependent (BOLD) signal time series within each of the 68 regions. Given that effects of tasks in functional-connectivity structure are small (18, 44), we included all functional MRI data from the three viewing conditions to minimize the possible effects from specific stimuli (e.g., specific to faces). Thus, subsequently, the BOLD signal time-series of each block was obtained and then mean-centered and detrended. We then concatenated the BOLD signal time-series of all blocks. Homotopic functional connectivity

was derived by calculating the Fisher Z-transformed Pearson correlation coefficients between the concatenated BOLD signals of each pair of the left–right homotopic regions.

Hemispheric Differences in Cortical Thinning and Maturation of Thickness Asymmetry during Adolescence. To examine the differences in cortical thinning between the left and right homotopic regions, a two-sample paired *t* test was utilized with FDR correction for 34 pairs of regions. To assess whether individuals' profiles of thickness asymmetry became more similar to an adult asymmetry profile, an adult profile was first derived by averaging the thickness-asymmetry profiles of 221 young adults (age 22) from IMAGEN. This subsample of participants did not overlap with the 532 participants but had T1-weighted images acquired and processed with the same protocols. Then, we calculated individual–adult similarity by calculating Pearson correlation coefficients between each participant's thickness asymmetry profile and the adult profiles at each visit, and compared the individual–adult similarity of visit 1, visit 2, and visit 3 by two samples paired *t* test.

The Density of Neurotransmitter Receptors and the Hemispheric Differences in Cortical Thinning. The data on density of neurotransmitter receptors were obtained from a report (12) that collated data from a large number of PET studies involving altogether over 1,200 healthy adults (42% female, mean sample-size weighted age = 36.6 y. Detailed in Table 1 of ref. 12). This report provided the density of 19 unique neurotransmitter receptors and transporters in the 68 cortical regions of Desikan–Killiany atlas (12). The values of density of a receptor/transporter from more than one study were combined using a weighted average (weighted by sample size of studies) after scaling the density across 68 regions within studies. Then, each of the 19 receptors and transporters density was z-scored across the 68 regions to derive normalized density. The hemispheric differences in the density of each neurotransmitter receptor were defined as "Left–Right" and thus, positive value means higher density in the left than the right hemisphere (L > R). We then tested correlations between the profile of hemispheric differences in thinning (positive values mean more thinning in the left than the right side) and the hemispheric differences in the density of each neurotransmitter receptor/transporter using simple permutation tests, as well as permutation tests adjusting for spatial autocorrelation using BrainSMASH (45). In the simple permutation tests, for each neurotransmitter receptor/transporter, we 1) obtained the correlation coefficients between the hemispheric differences in thinning and the hemispheric differences in the density of each neurotransmitter receptor/transporter; 2) calculated permutated correlation coefficient using the permuted hemispheric differences in thinning and the density of receptor/transporter; 3) repeated step (2) 10,000 times to generate a null distribution of correlation coefficients; and 4) compared the observed correlation coefficient with the null distribution using a two-sided test (with FDR correction for 19 neurotransmitter receptors/transporters). In the permutation tests with adjustments for spatial autocorrelation, we used BrainSMASH to simulate 10,000 surrogate brain maps (null models) of the hemispheric differences in thinning with spatial autocorrelation that is matched to the spatial autocorrelation in original data. This was achieved in two main steps: 1) randomly permuted the values in the map of the hemispheric differences in thinning, and 2) smoothed and rescaled the permuted values to reintroduce spatial autocorrelation characteristic of the original data. We then calculated correlation coefficients between the surrogate brain maps of the hemispheric differences in thinning and the hemispheric differences in the density of each neurotransmitter receptor/transporter. We then obtained p values by comparing the observed correlation coefficient with the null distribution using a two-sided test. All statistical analyses were done with R (version 4.2.2). The brain maps were plot with R package "fsbrain".

Homotopic Functional Connectivity and Hemispheric Differences in Cortical Thinning. We assumed that regions with strong and stable homotopic functional connectivity would show similar age-related changes in cortical thickness between left and right regions during adolescence. Since homotopic functional connectivity is undirected, we used the absolute values of hemispheric differences in thinning and referred it as "absolute hemispheric differences in thinning". A higher value indicates a larger difference in thinning between left and right homotopic regions. Functional connectivity can be unstable and vary from time to time (19, 46). Thus, to capture the stable profile of functional connectivity throughout adolescence, we averaged the homotopic functional-connectivity profiles obtained in all three visits for each participant. The hypothesis was tested by correlating the profile of homotopic functional connectivity to the profile of absolute hemispheric differences in thinning at both group-average and individual levels using permutation tests (with and without spatial autocorrelation). For the group-level analysis, in the simple permutation tests, we compared the observed correlation coefficient with the null distribution derived from 10,000 permutations using a one-sided test as our hypothesis was formulated in a specific direction: absolute hemispheric differences in thinning correlate negatively with functional connectivity. In the permutation tests with spatial autocorrelation preserved, we used BrainSMASH to simulate 10,000 surrogate brain maps of the homotopic functional connectivity. We then compared the observed correlation coefficient with the null distribution of correlation between the absolute hemispheric differences in thinning and the 10,000 surrogate brain maps of functional connectivity. For the individual level, we calculated correlation coefficients between homotopic functional connectivity and absolute hemispheric differences in thinning for each individual. We then obtained the average of 5,000 permutated correlation coefficients between the shuffled homotopic functional connectivity (with and without spatial autocorrelation) and the absolute hemispheric differences in thinning for each individual. A paired *t* test was then performed to determine whether the observed correlation coefficients were significantly lower than the average of permutated correlation coefficients.

We then asked how the individual-shared and individual-specific part of functional connectivity contribute to the association between functional connectivity and the absolute hemispheric differences in thinning. To answer this question, we correlated each participant's profile of absolute hemispheric differences in thinning to the functional-connectivity profiles of all other participants (one by one), and then averaged the correlation coefficients as an interindividual correlation. The correlations between participant's profile of absolute hemispheric differences in thinning and their own functional connectivity were referred to as an intraindividual correlation. Two samples paired *t* test was used to compare the difference between the intraindividual and the interindividual correlations. Higher intraindividual than the interindividual correlation would be expected if there were a contribution of the individual-specific part of functional connectivity.

Lastly, we asked if regions with large hemispheric differences in the density of neurotransmitter receptors and transporters would show weak homotopic functional connectivity. Homotopic functional connectivity is undirected and brain activity is influenced by a balance of different neurotransmitter receptors (10). Thus, to quantify the undirected left–right differences in neurotransmitter receptor/transporter density, we summed up the absolute hemispheric differences of the 19 receptors and referred to this quantity as neurotransmitter difference. Thus, we obtained a profile of the (overall) neurotransmitter difference across the 34 regions, with the higher value indicating a larger difference across the neurotransmitter systems. We then tested whether regions with high left–right differences in the receptor density would have low homotopic functional connectivity using permutation tests (with and without spatial autocorrelation) with a one-sided test, as our hypothesis was formulated in a specific direction: receptor differences negatively correlate with functional connectivity. The permutation tests were done in the following steps: 1) obtaining the observed correlation coefficients between receptor differences and group-average functional connectivity; 2) permuting receptor differences and calculated a simulated correlation coefficient by correlating the resampled receptor differences to functional connectivity; 3) repeating step (2) 10,000 times to generate a null distribution of correlation coefficients; 4) comparing the observed correlation coefficient against the null distribution using a one-sided test. In the permutation tests with spatial autocorrelation, we compared the observed correlation coefficient with the null distribution of correlation between the receptor differences and the 10,000 surrogate brain maps of functional connectivity BrainSMASH.

Genes Coexpressed with Neurotransmitter Receptors/transporters. To explore potential biological functions of neurotransmitter receptor/transporters that had the strongest relationship with the hemispheric differences in cortical thinning, we conducted gene-ontology (GO) term analysis with coexpression genes of the neurotransmitter receptor/transporter genes. We selected the genes of the top 5 and bottom 5 neurotransmitter receptor/transporters with the strongest relationship with the hemispheric differences in cortical thinning (Table 1). The genes of the top 5 receptor/transporters included *GRIN1* (NMDA), *GRIN2A* (NMDA), *GRIN2B* (NMDA), *SLC6A3* (DAT), *OPRM1* (MOR), *SLC18A3* (VAChT), and *HTR1B* (HTRB). The

genes of the bottom 5 receptor/transporters included *HTR2A* (5HT2a), *SLC6A4* (5HTT), *DRD2* (D2), *CNR1* (CB1), *CHRNA4* ($\alpha4\beta2$), and *CHRNB2* ($\alpha4\beta2$). Using a linear mixed-effects model, we identified top 10 positively coexpressed genes of each receptor/transporter gene within a harmonized dataset of gene expression in cerebral cortex. This dataset included 16,245 genes from 534 donors aged 0 to 102 y from Allen Human Brain Atlas, BrainCloud, the Brain eQTL Almanac, the Genotype-Tissue Expression Project, and BrainSpan (30). Age, hemisphere, and sex were considered as fixed effects, while region and donor ID were treated as random effects in the mixed-effects model. The coexpressed genes for each receptor/transporter gene were used to construct the top and bottom neurotransmitter receptor/transporters coexpressed panels. We then conducted GO enrichment analysis on these two gene lists using the "clusterProfiler" R package (47). Only GO terms with a minimum of 10, and maximum of 500 genes were tested, and redundant terms were removed with a similarity cut-off of 0.7 (default parameters).

Data, Materials, and Software Availability. Data are available upon request via IMAGEN: https://imagen-project.org/the-imagen-dataset/ (20).

ACKNOWLEDGMENTS. We thank Chunhui Hao for his helpful comments and inspiration. We also thank Manon Bernard, Steven Tilley, and Daniel Vosberg for their help in analyzing MRI data, gene coexpression, and checking grammar. This research was specifically funded by Wellcome Trust and MRC (076467/Z/05/Z). IMAGEN received support from the following sources: the European Union-funded FP6 Integrated Project IMAGEN (Reinforcement-related behaviour in normal brain function and psychopathology) (LSHM-CT- 2007-037286), the Horizon 2020 funded ERC Advanced Grant "STRATIFY" (Brain network based stratification of reinforcement-related disorders) (695313), Human Brain Project (HBP SGA 2, 785907, and HBP SGA 3, 945539), the Medical Research Council Grant "Consortium on Vulnerability to Externalizing Disorders and Addictions" (MR/N000390/1), the NIH (R01DA049238, A decentralized macro and micro gene-by-environment interaction analysis of substance use behavior and its brain biomarkers), the National Institute for Health Research Biomedical Research Centre at South London and Maudsley NHS Foundation Trust and King's College London, the Bundesministeriumfür Bildung und Forschung (BMBF grants 01GS08152; 01EV0711; Forschungsnetz AERIAL 01EE1406A, 01EE1406B), the Deutsche Forschungsgemeinschaft (DFG grants SM 80/7-2, SFB 940, TRR 265, NE 1383/14-1), the Medical Research Foundation and Medical Research Council (grants MR/R00465X/1 and MR/S020306/1), the NIH funded ENIGMA (grants 5U54EB020403-05 and 1R56AG058854-01). Further support was provided by grants from the ANR (ANR-12-SAMA-0004, AAPG2019–GeBra), the Eranet Neuron (AF12-NEUR0008-01–WM2NA; and ANR-18-NEUR00002-01–ADORe), the Fondation de France (00081242), the Fondation pour la Recherche Médicale (DPA20140629802), the Mission Interministérielle de Lutte-contre-les-Drogues-et-les-Conduites-Addictives (MILDECA), the Assistance-Publique-Hôpitaux-de-Paris and INSERM (interface grant), Paris Sud University IDEX 2012, the Fondation de l'Avenir (grant AP-RM-17-013), the Fédération pour la Recherche sur le Cerveau; the NIH, Science Foundation Ireland (16/ERCD/3797), U.S.A. (Axon, Testosterone and Mental Health during Adolescence; RO1 MH085772-01A1), and by NIH Consortium grant U54 EB020403, supported by a cross-NIH alliance that funds Big Data to Knowledge Centres of Excellence. This research was supported by a grant from the NIH (R01MH085772 to T. Paus). This publication is the work of the authors and T.P. will serve as guarantors for the contents of this paper and does not necessarily represent the official views of the NIH.

Author affiliations: [a]Research Centre of Sainte-Justine University Hospital, Montreal, QC H3T 1C5, Canada; [b]Department of Psychiatry and Addictology, University of Montreal, Montreal, QC H3T 1J4, Canada; [c]Department of Child and Adolescent Psychiatry and Psychotherapy, Central Institute of Mental Health, Medical Faculty Mannheim, Heidelberg University, Mannheim 68159, Germany; [d]Discipline of Psychiatry, School of Medicine, Trinity College Dublin, Dublin D02 PN40, Ireland; [e]Trinity College Institute of Neuroscience, Trinity College Dublin, Dublin D02 PN40, Ireland; [f]Centre for Population Neuroscience and Precision Medicine, Institute of Psychiatry, Psychology & Neuroscience, Social, Genetic & Developmental Psychiatry Centre, King's College London, London SE5 8AF, United Kingdom; [g]Institute of Cognitive and Clinical Neuroscience, Central Institute of Mental Health, Medical Faculty Mannheim, Heidelberg University, Mannheim 69117, Germany; [h]Department of Psychology, School of Social Sciences, University of Mannheim, Mannheim 68131, Germany; [i]NeuroSpin, Energies and Atomic Energy Commission, Université Paris-Saclay, Paris F-91191, France; [j]Department of Psychiatry, University of Vermont, Burlington, VT 05405; [k]Department of Psychology, University of Vermont, Burlington, VT 05405; [l]Sir Peter Mansfield Imaging Centre School of Physics and Astronomy, University of Nottingham, Nottingham NG7 2RD, United Kingdom; [m]Department of Psychiatry and Psychotherapy, Campus Charité Mitte, Charité, Universitätsmedizin Berlin, Berlin 10117, Germany; [n]Physikalisch-Technische Bundesanstalt, Braunschweig and Berlin 38116, Germany; [o]Institut National de la Santé et de la Recherche Médicale, INSERM U1299 "Developmental trajectories & psychiatry" Université Paris-Saclay, Ecole Normale supérieure Paris-Saclay, CNRS, Centre Borelli, Paris 75006, France; [p]Department of Child and Adolescent Psychiatry, Pitié-Salpêtrière Hospital, AP-HP. Sorbonne Université, Paris 75006, France; [q]Etablissement Public de Santé Barthélemy Durand, Paris 91700, France; [r]Institute of Medical Psychology and Medical Sociology, University Medical Center Schleswig Holstein, Kiel University, Kiel 24118, Germany; [s]Department of Child and Adolescent Psychiatry and Psychotherapy, University Medical Centre Göttingen, Göttingen 37075, Germany; [t]Department of Psychiatry and Neuroimaging Center, Technische Universität Dresden, Dresden 01087, Germany; [u]School of Psychology and Global Brain Health Institute, Trinity College Dublin, Dublin D02 PN40, Ireland; [v]Centre for Population Neuroscience and Precision Medicine, Institute of Psychiatry, Psychology & Neuroscience, Institute for Science and Technology of Brain-inspired Intelligence, Fudan University, Shanghai 200437, Peoples Republic of China; [w]Centre for Population Neuroscience and Precision Medicine, Charite Universitätsmedizin Berlin, Berlin 10117, Germany; and [x]Department of Neuroscience, University of Montreal, Montreal, QC H3T 1J4, Canada

Author contributions: Z.L., T.B., A.L.W.B., S.D., H.F., A.G., H.G., P.G., A.H., B.I., J.-L.M., M.-L.P.M., E.A., F.N., D.P.O., L.P., S.H., S.M., J.H.F., M.N.S., H.W., R.W., G.S., T.P., and I.C. designed research; Z.L., T.B., A.L.W.B., S.D., H.F., A.G., H.G., P.G., A.H., B.I., J.-L.M., M.-L.P.M., E.A., F.N., D.P.O., L.P., S.H., S.M., J.H.F., M.N.S., H.W., R.W., G.S., T.P., and I.C. performed research; Z.L. analyzed data; and Z.L. and T.P. wrote the paper.

Competing interest statement: T.B. served in an advisory or consultancy role for eye level, Infectopharm, Lundbeck, Medice, Neurim Pharmaceuticals, Oberberg GmbH, Roche and Takeda. He received conference support or speaker's fee by Janssen, Medice and Takeda. He received royalties from Hogrefe, Kohlhammer, CIP Medien, Oxford University Press. The present work is unrelated to the above grants and relationships. The other authors report no biomedical financial interests or potential conflicts of interest.

1. V. Duboc, P. Dufourcq, P. Blader, M. Roussigné, Asymmetry of the Brain: Development and Implications. *Annu. Rev. Genet.* **49**, 647–672 (2015).
2. N. Geschwind, A. M. Galaburda, Cerebral lateralization., Biological mechanisms, associations, and pathology: I. A hypothesis and a program for research. *Arch. Neurol.* **42**, 428–459 (1985).
3. A. W. Toga, P. M. Thompson, Mapping brain asymmetry. *Nat. Rev. Neurosci.* **4**, 37–48 (2003).
4. G. Li, W. Lin, J. H. Gilmore, D. Shen, Spatial patterns, longitudinal development, and hemispheric asymmetries of cortical thickness in infants from birth to 2 years of age. *J. Neurosci.* **35**, 9150–9162 (2015).
5. P. Shaw *et al.*, Development of cortical asymmetry in typically developing children and its disruption in attention-deficit/hyperactivity disorder. *Arch. Gen. Psychiatry* **66**, 888–896 (2009).
6. D. Zhou, C. Lebel, A. Evans, C. Beaulieu, Cortical thickness asymmetry from childhood to older adulthood. *Neuroimage* **83**, 66–74 (2013).
7. M. C. Postema *et al.*, Analysis of structural brain asymmetries in attention-deficit/hyperactivity disorder in 39 datasets. *J. Child Psychol. Psychiatry* **62**, 1202–1219 (2021).
8. J. M. Huntenburg, P.-L. Bazin, D. S. Margulies, Large-scale gradients in human cortical organization. *Trends Cogn. Sci.* **22**, 21–31 (2018).
9. D. D. Larsen, L. Krubitzer, Genetic and epigenetic contributions to the cortical phenotype in mammals. *Brain Res. Bull* **75**, 391–397 (2008).
10. K. Zilles *et al.*, Architectonics of the human cerebral cortex and transmitter receptor fingerprints: Reconciling functional neuroanatomy and neurochemistry. *Eur. Neuropsychopharmacol.* **12**, 587–599 (2002).
11. K. Zilles, M. Bacha-Trams, N. Palomero-Gallagher, K. Amunts, A. D. Friederici, Common molecular basis of the sentence comprehension network revealed by neurotransmitter receptor fingerprints. *Cortex* **63**, 79–89 (2015).
12. J. Y. Hansen *et al.*, Mapping neurotransmitter systems to the structural and functional organization of the human neocortex. *Nat. Neurosci.* **25**, 1569–1581 (2022).
13. B. Draganski *et al.*, Neuroplasticity: Changes in grey matter induced by training. *Nature* **427**, 311–312 (2004).
14. J. Driemeyer, J. Boyke, C. Gaser, C. Buchel, A. May, Changes in gray matter induced by learning–revisited. *PLoS One* **3**, e2669 (2008).
15. R. J. Zatorre, R. D. Fields, H. Johansen-Berg, Plasticity in gray and white: Neuroimaging changes in brain structure during learning. *Nat. Neurosci.* **15**, 528–536 (2012).
16. K. L. Hyde *et al.*, Musical training shapes structural brain development. *J. Neurosci.* **29**, 3019–3025 (2009).
17. A. Raznahan *et al.*, Patterns of coordinated anatomical change in human cortical development: A longitudinal neuroimaging study of maturational coupling. *Neuron* **72**, 873–884 (2011).
18. C. Gratton *et al.*, Functional brain networks are dominated by stable group and individual factors, not cognitive or daily variation. *Neuron* **98**, 439–452.e5 (2018).
19. Z. Liao *et al.*, Similarity and stability of face network across populations and throughout adolescence and adulthood. *NeuroImage* **244**, 118587 (2021).
20. G. Schumann *et al.*, The IMAGEN study: Reinforcement-related behaviour in normal brain function and psychopathology. *Mol. Psychiatry* **15**, 1128–1139 (2010).
21. R. S. Desikan *et al.*, An automated labeling system for subdividing the human cerebral cortex on MRI scans into gyral based regions of interest. *Neuroimage* **31**, 968–980 (2006).
22. X.-Z. Kong *et al.*, Mapping cortical brain asymmetry in 17,141 healthy individuals worldwide via the ENIGMA Consortium. *Proc. Natl. Acad. Sci. U.S.A.* **115**, E5154–E5163 (2018).
23. E. Bullmore, O. Sporns, Complex brain networks: Graph theoretical analysis of structural and functional systems. *Nat. Rev. Neurosci.* **10**, 186–198 (2009).

24. V. J. Sydnor *et al.*, Neurodevelopment of the association cortices: Patterns, mechanisms, and implications for psychopathology. *Neuron* **109**, 2820–2846 (2021).
25. D. Schijven *et al.*, Large-scale analysis of structural brain asymmetries in schizophrenia via the ENIGMA consortium. *Proc. Natl. Acad. Sci. U.S.A.* **120**, e2213880120 (2022), 10.1101/2022.03.01.22271652.
26. A. Shapson-Coe *et al.*, A connectomic study of a petascale fragment of human cerebral cortex. bioRxiv [Preprint] (2021). https://doi.org/10.1101/2021.05.29.446289 (Accessed 21 March 2023).
27. N. Palomero-Gallagher, K. Zilles, Cortical layers: Cyto-, myelo-, receptor- and synaptic architecture in human cortical areas. *NeuroImage* **197**, 716–741 (2019).
28. H. T. Cline, Dendritic arbor development and synaptogenesis. *Curr. Opin. Neurobiol.* **11**, 118–126 (2001).
29. H.-B. Kwon, B. L. Sabatini, Glutamate induces de novo growth of functional spines in developing cortex. *Nature* **474**, 100–104 (2011).
30. N. Parker *et al.*, Assessment of neurobiological mechanisms of cortical thinning during childhood and adolescence and their implications for psychiatric disorders. *JAMA Psychiatry* **77**, 1127–1136 (2020).
31. T. Paus, Mapping brain maturation and cognitive development during adolescence. *Trends Cogn. Sci.* **9**, 60–68 (2005).
32. T. Paus, Tracking development of connectivity in the human brain: Axons and dendrites. *Biol. Psychiatry* **93**, 455–463 (2022) 10.1016/j.biopsych.2022.08.019.
33. J. Shin *et al.*, Cell-specific gene-expression profiles and cortical thickness in the human brain. *Cereb. Cortex* **28**, 3267–3277 (2018).
34. R. D. Fields, A new mechanism of nervous system plasticity: Activity-dependent myelination. *Nat. Rev. Neurosci.* **16**, 756–767 (2015).
35. Z. Petanjek *et al.*, Extraordinary neoteny of synaptic spines in the human prefrontal cortex. *Proc. Natl. Acad. Sci. U.S.A.* **108**, 13281–13286 (2011).
36. C. Paquola *et al.*, Microstructural and functional gradients are increasingly dissociated in transmodal cortices. *PLoS Biol.* **17**, e3000284 (2019).
37. J. Seidlitz *et al.*, Morphometric similarity networks detect microscale cortical organization and predict inter-individual cognitive variation. *Neuron* **97**, 231–247.e7 (2018).
38. L. T. Eyler *et al.*, Conceptual and data-based investigation of genetic influences and brain asymmetry: A twin study of multiple structural phenotypes. *J. Cogn. Neurosci.* **26**, 1100–1117 (2014).
39. Z. Sha *et al.*, The genetic architecture of structural left-right asymmetry of the human brain. *Nat. Hum. Behav.* **5**, 1226–1239 (2021).
40. M. H. Grosbras, T. Paus, Brain networks involved in viewing angry hands or faces. *Cereb. Cortex* **16**, 1087–1096 (2006).
41. O. Esteban *et al.*, MRIQC: Advancing the automatic prediction of image quality in MRI from unseen sites. *PLoS One* **12**, e0184661 (2017).
42. O. Esteban *et al.*, fMRIPrep: A robust preprocessing pipeline for functional MRI. *Nat. Methods* **16**, 111–116 (2019).
43. J.-P. Fortin *et al.*, Harmonization of cortical thickness measurements across scanners and sites. *NeuroImage* **167**, 104–120 (2018).
44. M. W. Cole, D. S. Bassett, J. D. Power, T. S. Braver, S. E. Petersen, Intrinsic and task-evoked network architectures of the human brain. *Neuron* **83**, 238–251 (2014).
45. J. B. Burt, M. Helmer, M. Shinn, A. Anticevic, J. D. Murray, Generative modeling of brain maps with spatial autocorrelation. *NeuroImage* **220**, 117038 (2020).
46. L. Geerligs, M. Rubinov, Cam-Can, R. N. Henson, State and trait components of functional connectivity: Individual differences vary with mental state. *J. Neurosci.* **35**, 13949–13961 (2015).
47. T. Wu *et al.*, clusterProfiler 4.0: A universal enrichment tool for interpreting omics data. *Innovation (Camb)* **2**, 100141 (2021).